AAS 97 -735

THE ASTRODYNAMICS OF NEW PLANETARY SYSTEMS: THE ELLIPTIC RESTRICTED 3-BODY PROBLEM

W. D. Kelly [1]

Elliptic Restricted 3-Body Problem (ER3BP) simulations illustrate measures of relative stability for extra-solar planets, using terrestrial analogs as 3rd bodies in binary systems α Centauri, Procyon, Sirius, Jupiter-Sun, 47 Ursae Majoris and 70 Virginis. Initial conditions placed hypothetical planets in nominally circular orbits at Earth analogous radiative flux regions (400^o K effective stellar temperature at orbital radius), plus increments above and below. As tracked for 10^3 - 10^5 years, secondary bodies (star, brown dwarf or planet) perturbed nominally circular, co-planar planetary orbits at pericentron passage, causing eccentricity and angular momentum to cycle from 10^2 to 10^5 years as planet periastron precessed. Cases include satellites of jovian planets or brown dwarfs. Cycle magnitudes and periods varied with star system case and thermal environment. In some instances, stable orbit bounds were established by capture, ejection or advent of chaotic motions. Effective temperature bounds of stable regions varied with each binary system. For calibrating detection projects, observations of Earth from deep space are suggested.

Introduction

Search for extra-solar planet orbits stable for life resembles the astrodynamics problem of satellite mission orbit selection. In the extra-solar problem, analysts deal with primary body gravity, radiation and, in many cases, a secondary perturbing body, whether a star, giant planet or brown dwarf. Since 1985, we have analyzed [1-2] planetary stability for nearby binary stars (α Centauri, Sirius, Procyon) as an Elliptic Restricted 3-Body Problem (ER3BP) for mean stellar separations $20 < a^* < 30$ AU and eccentricity $0 < \mathbf{e} < 0.6$. Planet orbits thermally analogous to Earth's (T_{eff} at orbital radius ~ 400^o K) were initialized and tracked for 10^4 -10^5 years, along with objects in other temperature (200-500^o K) zones. Secondary stars perturbed nominally circular, co-planar planetary orbits at stellar pericentron passage, causing **e** and angular momentum to cycle over ~10^3 years as planet periastron position $\boldsymbol{\omega_p}$ precessed. Our primary example, a planet of α Centauri A illustrates this in Figs 1-3, perturbed by α Centauri B, a K1v Main Sequence star, fainter and less massive than the Sun (Table-1). With recent Doppler or visual detections [3,4] of jovian or brown dwarf partners to stars at radii where terrestrial planets are preferred (47 Ursae Majoris, 70 Virginis...), ER3BP studies include new binary cases and data (Tables 1- 3). With accelerations proportional to M/R^2, despite less mass, "planetary" cases appear similar to "stellar" cases due to closer proximity. Binary system comparisons show that regions where planets are unstable or ejected vary in T_{eff} - affecting available proto-planetary chemical constituents. Stable orbit regions also possess "quantum" properties; angular momentum states appear to increment each periastron or be bound to cycles until "transition" perturbations occur. Thus, terrestrial planets, if extant near binaries, experience (in ER3BP 4th-order Runge-Kutta integration) complex climate cycles influenced by secondary bodies. Observed environments provide different (than solar) formation circumstances, whether processes are accelerated or inhibited.

[1]Aerospace Consultant, Triton Systems, 15902 Spring Forest, Houston, TX 77059-3811
E-mail: kelly@lock.jsc.nasa.gov

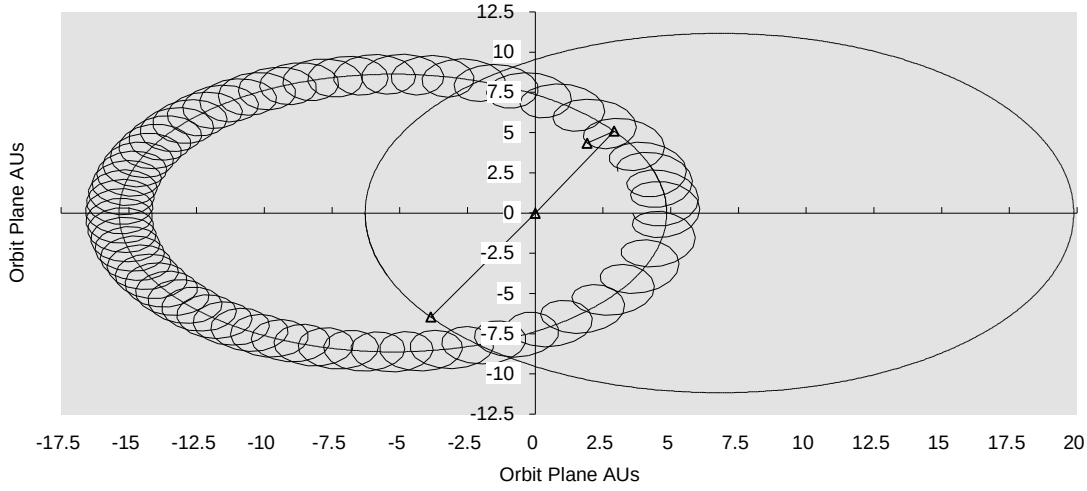

Fig.-1 α Centauri A and B with Planetary Track, Epoch =1,500 Days, Origin at Barycenter Inertial Coordinates, Mean Separation a* = 23.4 AU, e* = .52, P* = 79.9 yrs
Stellar Mass: $M_A = 1.1$, $M_B = .85$, Luminosity: $L_A = 1.5$, $L_B = .40$ (Solar Units)

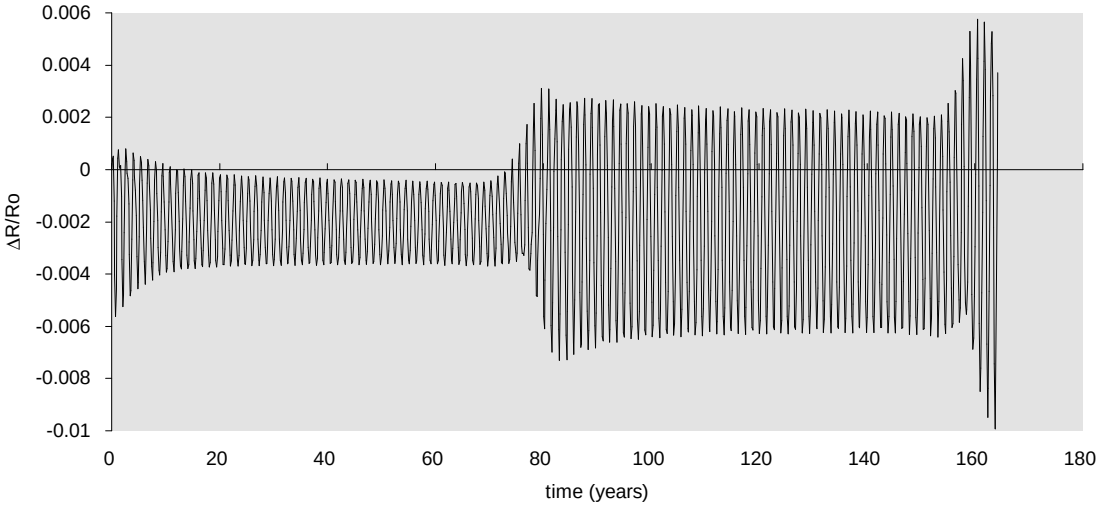

Fig.-2 α Centauri A Planetary Orbit Perturbation over 160 Years or 2 Stellar Revolutions
$R_o = 1.2468$ AU, $T_{eff} = 400^o$ K, P = 486 days, P* = 79.9 yrs

Background

A large fraction of the nearest stars reside in binary systems. More distant stars are often subsequently resolved into visual or spectroscopic binaries, some of the smallest recently discovered components possessing less than "stellar" mass. Parallax measure for the nearest star system is 0.743 arcsecs. An arc second shift represents a distance of 206,264.8 AUs (1 parsec); thus, the 1.34 parsec or 4.43 light-year

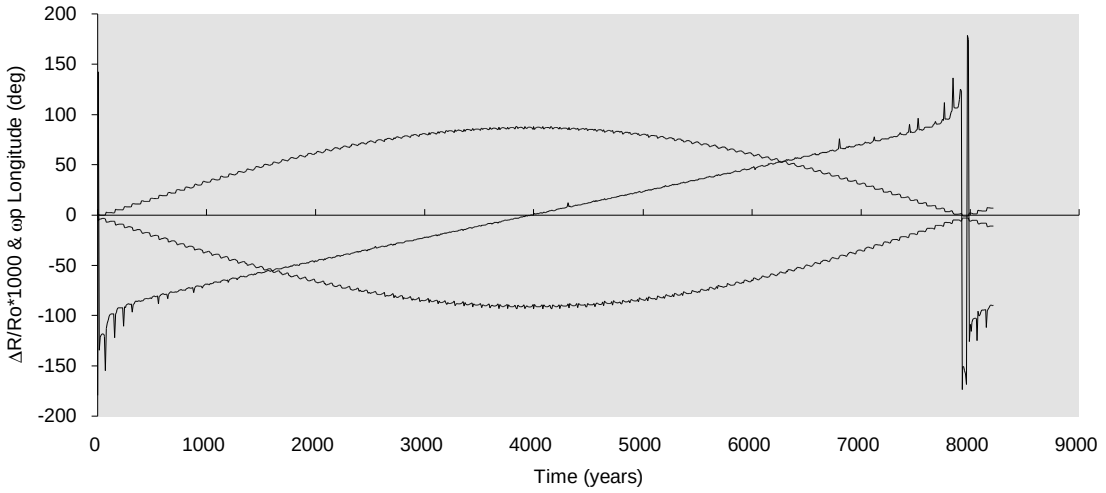

Fig.-3 α Centauri A Planet ($\Delta R/R_o$) Max, Min and ω_p over ~100 Stellar Revolutions
R_o = 1.2468 AU, T_{eff} = 400^o K, P= 486 days, P*=79.9 yrs.

distance to α Centauri represents 282,554 AUs. With 1 AU = 1.4959x10^8 km and 380,000 km separating Earth and Moon, the nearest interstellar neighbors lie 8 orders of magnitude farther off. How such distances can be traversed within a human lifetime by spacecraft is not now readily apparent, yet as Fig. 1 shows, binary systems pose problems enough for navigation on arrival. Since 1995, with the discovery of jovian or greater mass (>M_J) objects in orbit near several different stars, an open question remains whether descending hierarchies of other objects exist - terrestrial mass (M_E) planets or Galilean moons - in stable orbits within these binary systems. Perhaps less dramatic, but no less significant, are circumstellar disks (CSDs) [5,6], commonly associated with infrared emission excesses in pre-Main Sequence stars. Since CSDs in theory last 10^7 years and early phase planet formation requires ~10^5, for young (T Tauri) stars in the Hyades, Taurus and Orion constellations, planet formation offers explanation for CSD differentiation and gaps. Observers suspect one or two Jupiter-sized planets embedded in the disk of β Pictoris, responsible for disk warping and transitory spectroscopic events.

Despite analogies drawn to satellite placement, some extra-solar planetary detection and analysis problems are quite distinct from conventional astrodynamics. Binary systems within parallax measure-ment limits provide most of the direct evidence for stellar mass and luminosity (M* and L*, solar units) supporting astrophysical theory. Stars at greater distance in associated clusters receive M* and L* estimates based on spectral analysis and position in the Hertzsprung-Russell diagram of color and brightness, corresponding to effective surface temperature (T^*_{eff}) and L*, and less directly, M*, elemental composition and age. Astrophysical theory for these classifications is described in [7,8,9]; the observational values used for our simulations were taken from descriptive catalogs [10,11], or provided in extra-solar planet discovery reports [3,4]. For binaries, spectroscopic measurements provide stellar line of sight (LOS) velocity shifts, but these do not directly account for orbital plane angle with respect to the observer. Evidence such as detected eclipses or spectral line features due to stellar rotation must be taken into account for inclination assessments. Visible or IR data are generally noisy at current sensitivities due to low Doppler shifts, and the relatively broad, fuzzy nature of observed spectral lines. In contrast, pulsar radio emissions are sharp signals measured accurately enough to detect planet-like bodies with orbits and masses similar to Earth's. The overall results of visual Doppler are uncertainties in local gravitational fields, mean separations and other parameters. Thus, simulation values should be considered representative, but not entirely arbitrary (i.e., high significant numbers return formula input values).

Planetary stability studies originated with the Solar System to determine if planets remain stable over eons in configurations beside that observed. A "New Earth" orbiting a single star is a non-issue, but planetary theory suggests that from the collapse of a proto-planetary cloud surrounding an isolated star several gas giant planets would form. Serious planetary stability studies now include binary star systems and systems with substellar companions, whether brown dwarfs or of Jupiter mass. Consequently the Jupiter-Sun-Planet system becomes an endpoint in our own spectrum of ER3BP cases, illustrated by Earth and Mars compared to the α Centauri case in Fig.4.

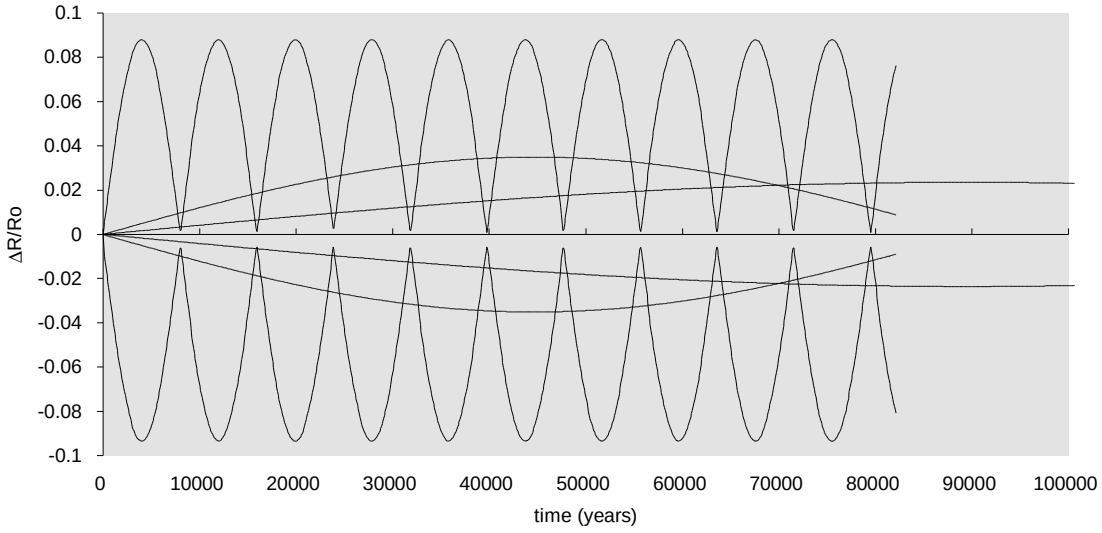

Fig.-4 ER3BP Planetary Orbit Perturbations for Earth, Mars and α Centauri A Planet, Eccentricity Periods in Descending Order. Current Earth and Mars Eccentricity .016722 and .093377.

Simulation of our well-observed Solar System poses problems enough and illustrates the dilemmas of new system analysis. For Solar System endeavors, analysts use various simulation fidelity levels. A common approach is to extrapolate from tables the changing orbital elements of the planets and integrate motions with respect to a fixed Sun for navigating spacecraft to rendezvous targets in mission studies. In the case of an Earth-Moon-Spacecraft problem, the Restricted 3-Body Problem (R3BP) assumes that the two principal bodies rotate about barycenter at constant rate with zero **e** and spacecraft mass remains negligible. To a certain level the Solar System can be approximated by the basic Sun-Jupiter R3BP with all other objects as negligible as spacecraft; in this system the Sun orbits the inertial barycenter in a near 12 year cycle with a radius of 0.001 of Jupiter's 5.2 AU distance: 765,000 km. This generates a 12m/s tangential velocity component. Conversion to ER3PB requires accounting for Jupiter $\mathbf{e}^*$=0.048. But Solar System bodies constitute significant masses themselves, starting with Saturn (.2994 M_J). In actuality the Sun's rotation about barycenter, though dominated by Jupiter, becomes an irregular wandering. N-body integration is needed to extrapolate this motion. In recent years with improvements in computational facilities and algorithms, Solar System n-body simulations have been conducted to cover even 10^9 years of future motion or previous history. These same techniques can be, and are, applied to other star systems as well, though with hypothetical third planet bodies - for the time being.

Solar motion irregularities of ~12m/s could be detected by interstellar counterparts to terrestrial astronomers, providing technology "there" is as sensitive as "here" in the mid 1990s (e.g., [12]) at 10-15 parsecs distance. Objects discovered thus far by visual Doppler studies have had higher shifts than exerted by Jupiter and shorter orbital periods. Objects with periods as long as Jupiter's have been detected (or suspected) as a result of astrometric studies, watching for decade-long oscillations in stellar celestial coordinates. In either case, filtering out solar system and terrestrial distortions poses significant problems. Visually (or IR) detected Gliese 229B with separation of 40 AUs has no orbital elements to date.

Stellar binaries separated by Solar System dimensions frequently possess large (~0.5) **e** and some large planets or substellar companions detected thus far possess similar characteristics. For this reason the ER3BP can be employed for analyses of third bodies, objects which could be analogs of Earth. Our interest here is primarily (and justifiably) in terrestrial analogs; however, when one considers the constraints of constructing analogs in eccentric binary systems with differing radiation characteristics due to stellar luminosity, evolutionary history or emission peak wavelength, it is probable that New Earth would differ significantly from Old in geology, seismology and atmospheric evolution, not to mention biology.

Astrodynamic and Thermodynamic Relations Supporting the Data Base

Dynamic stability of habitable planets cannot be addressed without discussion of stellar flux characteristics and system dimensions; otherwise strict mathematical analysis of the canonical ER3BP will be diverted to regions too far from or too close to the primaries. Table-1 describes nearby binaries we have studied for several years, the Jupiter-Sun model (included for comparisons) and (the first few) recently discovered stars with brown dwarf or jovian planet partners. Each system creates interesting dynamic and thermodynamic environments for terrestrial planets. The basic formulas applied to this analysis are discussed briefly below.

Astrodynamics: Equations of Motion

For objects M_A and M_B with non-negligible mass ratios, the inertial point of reference is the barycenter about which the binary components revolve in proportional conics. Disregarding observational issues, the implicit Newtonian revision to Keplerian relations for stellar period P* is proportional to mean separation a* and the mass of the two primary bodies. G is the universal gravitational constant.

$$G (M_A + M_B) P^{*2} = (2\pi)^2 a^{*3} \qquad (1)$$

In the inertial coordinate system, illustrated by Fig.-1, the two objects follow conics with the same true anomaly f, eccentricity and opposing orientations ($e_A = e_B$, $f_A = f_B$, but clocked 180^o apart about barycenter) with dimensions inversely proportional to mass.

.

$$a^* = a_A + a_B \quad \text{and} \quad a_A / a_B = M_B / M_A \qquad (2a\&b)$$

$$r^*_A = a_A (1 - e_A^2) / (1 + e_A \cos f_A); \quad r^*_B = a_B (1 - e_B^2) / (1 + e_B \cos f_B) \qquad (3a\&b)$$

For a 3rd body of negligible mass (terrestrial planet, debris, or spacecraft vs. star), software integrates the gravitational accelerations $\underline{a}_{pl}$ in an inertial system to determine position ($\underline{R}_{Apl}$, $\underline{R}_{Bpl}$) and velocity.

$$\underline{a}_{pl} = GM_A/R_{Apl}^3 \, \underline{R}_{Apl} + GM_B/R_{Bpl}^3 \, \underline{R}_{Bpl} \qquad (4)$$

Here, we use a 4th order Runge-Kutta algorithm; others elsewhere, perhaps a symplectic scheme [13,14]. For primary mass position, the Kepler equation is solved at time t, interwoven into the R-K integration.

Observer conventions for binary system inclination sets 0^o with orbital plane normal aligned to LOS. An Earth observer of a spectroscopic binary has no direct measure of LOS inclination other than an eclipse. Eccentricity can be discerned from velocity shifts, but even for a circular orbit, LOS velocity remains proportionally sinusoidal for all inclinations; without position shifts, Doppler velocity shifts represent a family of solutions for the same P*. If the primary's place on the H-R diagram is identified, its mass uncertainty can be small. The invisible secondary, however, achieves its perturbing velocity on M_A with $M_B \sin i$. Fig. -5 shows that high mass values for low inclination systems can change the nature of M_B from a planet to a deuterium burning brown dwarf (13 M_J) or even a low mass hydrogen burning star (70 M_J or 0.07 M_{SUN}). These thresholds have significance for both 47 Ursae Majoris and 70 Virginis. Beside being more massive gravitational perturbers to terrestrial planets (Fig.-6 for 70 Virginis), they become

significant sources of thermal energy derived from nuclear processes. We can expect many gas giant planets to possess higher effective temperatures than implied by position relative to a primary body.

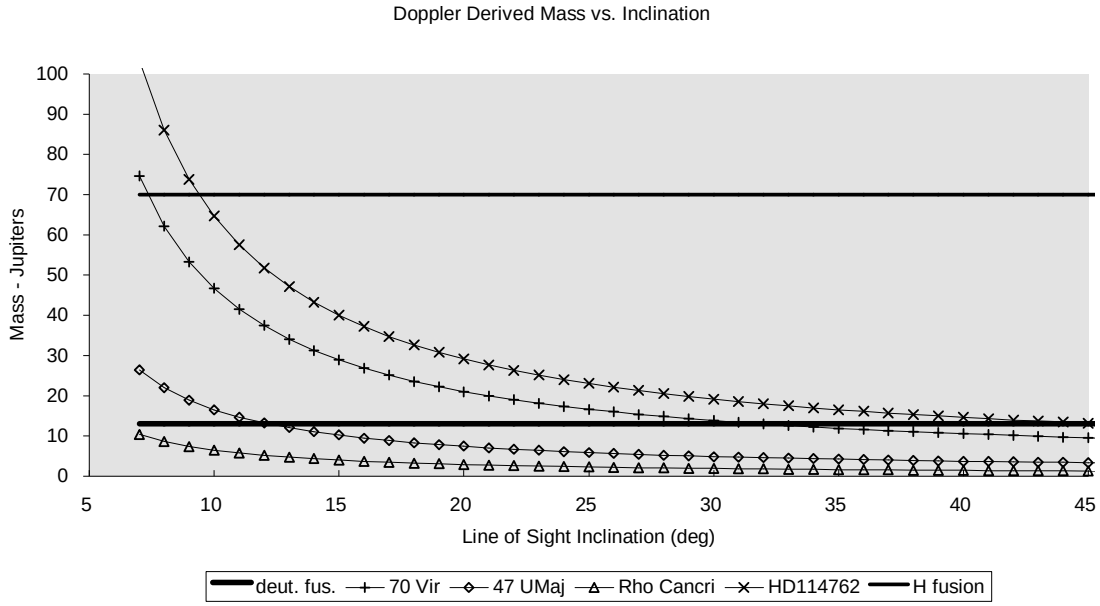

Fig.-5 Assumed Orbital Plane LOS Inclination - Effect on Mass Estimates
For Doppler Observed Secondary Bodies 70 Virginis, 47 Ursa Majoris, ρ Cancri, HD 114762
Thresholds for Deuterium and Hydrogen Fusion at 13 M_J and 70 M_J Respectively

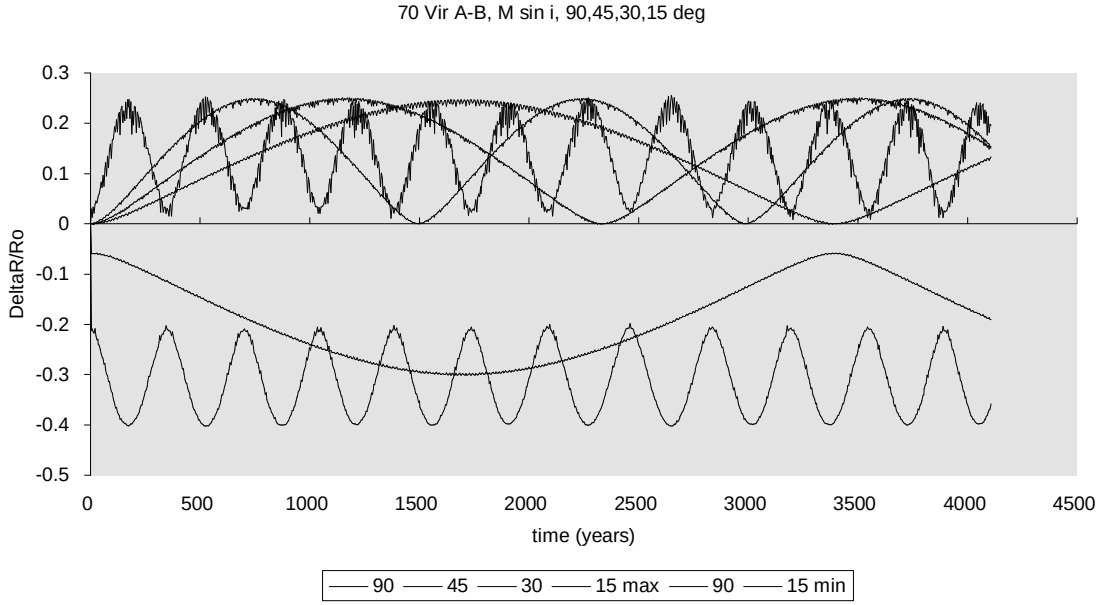

Fig.-6 70 Virginis A-B M_B sin i Effects for 90, 45, 30 and 15° Orbital Plane LOS Inclination

Thermodynamics: The Effects of the Equations of State

The stellar luminosity function of surface radius R* and effective surface temperature T^*_{eff} is the fundamental tool for determining where an earth analog should be placed with respect to another star.

$$L^* = 4\,\sigma\pi R^{*2}\,T^{*4}_{eff} \qquad (5)$$

Here σ is the Stefan-Boltzmann constant (5.6697×10^{-4} erg ^{o} K^{-4} cm^{-2} sec^{-1}). It is possible to estimate planetary temperature T_{pl} based on the illumination of two stars as a function of R*, T^*_{eff} and radial distances (R_{Ap1} and R_{Bpl}), plus planetary albedo A_{pl} with rapid rotation of the planet circulating thermal energy.

$$T_{pl}^4 = [\, T^{*4}_{A\,eff} (R^*_A/R_{Apl})^2 + T^{*4}_{B\,eff} (R^*_B/R_{Bpl})^2 \,] (1-A_{pl}) / 4 \qquad (6)$$

For our examples, the secondary object's gravity is more significant than its radiation, except for its direct satellites or planets. Moreover, for some terrestrial planets (Venus) A_{pl} can be misleading about surface temperatures below cloud layers. To eliminate A_{pl} , we consider the effective temperature of the Sun *at Earth's orbital radius* as about 400^{o} K (~1,370 watts/m^2 radiance based on solar T^*_{eff} ~5800^{o}) and seek similar lines in other star systems, solving for orbital radius R_{pl} where T_{eff} = 400^{o} K based on stellar flux.

$$T_{eff}(R_{pl}) = 400^{o}\,K = T^*_{eff}\,(R^*/R_{pl})^{0.5} \qquad (7)$$

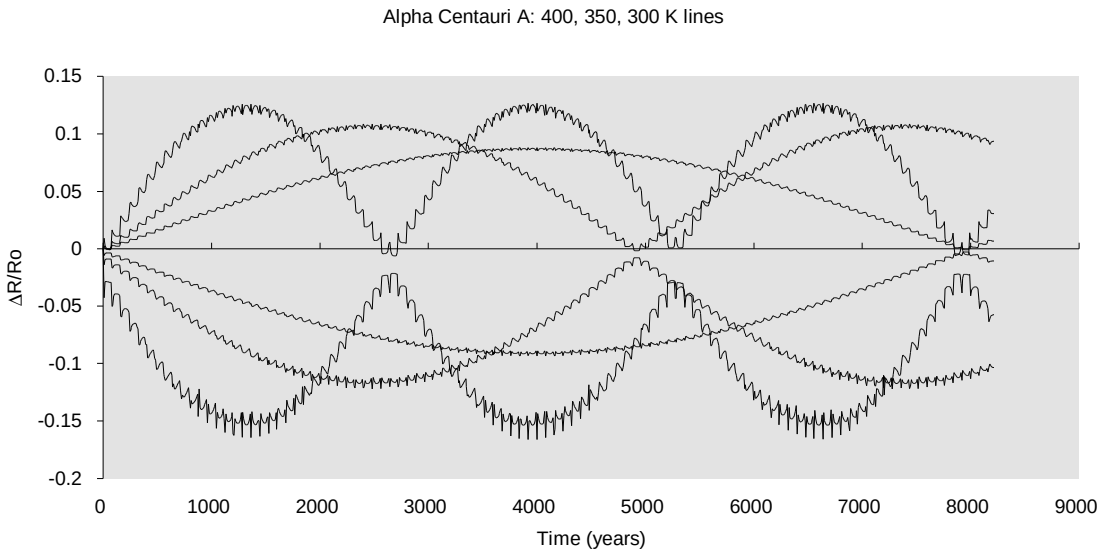

Fig.-7 α Centauri A Integration Data for T_{eff}=400, 350 and 300^{o} K (R_o =1.2468, 1.6825, 2.2165 AU) Transition to Instability and Ejection from Radii 2.0 to 2.75 (~T_{eff} = 225^{o} K)

Beside large variations in stellar flux due to T^*_{eff}, the quality of radiation varies with T^*_{eff} according to the Wien relation for wavelength λ_{max} of maximum emission.

$$\lambda_{max}\,T^*_{eff} = 0.290\ cm\ ^{o}K \qquad (8)$$

Fig.-8 illustrates this relation in which black-body Planck Function curves are normalized to peak wavelength values, approximating emission characteristics of several different T^*_{eff} stars of corresponding spectral classifications, scaled (roughly) for flux. Real star spectra include absorption and emission bands that often significantly distort the curves and complicate T^*_{eff} estimates. Of course, discrete bands are also sources of thermal, dynamic (Doppler) and chemical composition data. Peak emission for Sirius A is about 300 nanometers vs. 500 nm for the Sun. Beside pushing a planet nearly 5 times farther (4.88 AU) than

Earth from Sun for $T_{eff} = 400^o$, Sirius generates much more UV radiation for the same local T_{eff}. Yet by contrast, T^*_{eff} for Gl 229B, a probable brown dwarf [15], is ~1,000° K, suggesting that a 400° K envelope could surround it at ~400,000 km radius, though its radiation peaks in the IR. Kasting et al. examine the UV radiation effects of hotter and cooler stars in [16].

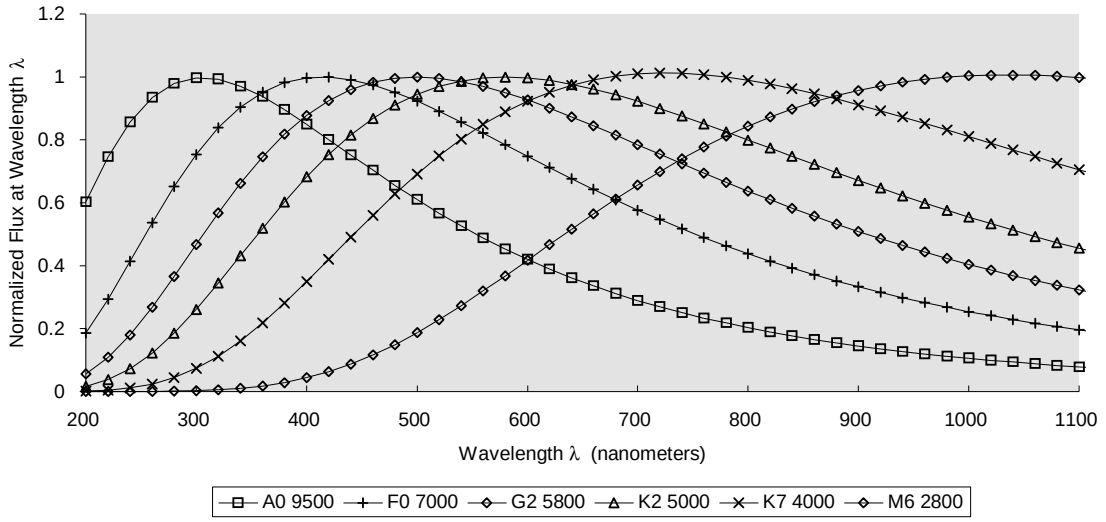

Fig.-8 Black Body (Planck Function) Radiation Curves Normalized to Peak Emission Wavelengths 5800° K T_{eff} Curve for G2 Star Peaks at 500 nm; 9500° K Curve for A0 Star at 300 nm

Using these thermodynamic and dynamic relations, we have constructed computer models for binary systems in which extra-solar terrestrial planets might reside. The primary stars are of similar spectral classification to the Sun (Main Sequence, G0v, G2v, G5v), some hotter and cooler representatives, most notably Sirius (A1v) and Procyon (F5iv) with their white dwarf partners. These secondaries are about as massive as the sun, significantly hotter, but little larger than Earth surface radius (~10^{-2} R_{SUN}). The cooler secondaries, brown dwarfs and jovian planets, are modeled as roughly jovian radius ($0.1R_{SUN}$), but with $150^o < T^*_{eff} < 1{,}500^o$ K. α Centauri B is an instance in which the secondary is also a M.S. star. Stellar properties are based on equilibrium solutions of state equations, frequently incomplete observations or imprecise estimates of distance, luminosity, mass, chemical constituents or age for objects configured in states of hydrostatic equilibrium supplemented by hydrogen or deuterium fusion. Arbitrary bounds for the habitable and stable zone can be established with temperature incremented (400, 350, 300°...) search. Fig.-7 illustrates the changing cycles for the α Centauri case.

Stable Planetary Orbit Characteristics

Tables-2 & 3 provide parametric summaries of ER3BP simulations. Table-2 results show stability changes with respect to T_{eff} for initial orbit radius R_o; Table-3 shows how assumed inclination affects stellar systems. When plots (Fig.-7,8) illustrate Tables 2 & 3 summaries, one sees transition from easily recognizable cycles of "stable" orbits to less clear-cut cycles on the threshold of capture by the secondary, elongation, or ejection from the system. To detect long-term periodic behavior $(\Delta R/R_o)_{MAX}$ or $(\Delta R/R_o)_{MIN}$ requires sampling intervals longer than one orbital revolution. If orbit period is known a priori, sampling for periastron and apoastron passage can be performed every n orbits. Should the orbit evolve to a longer period with a larger semi-major axis, then spurious samples begin to enter extrema curves.

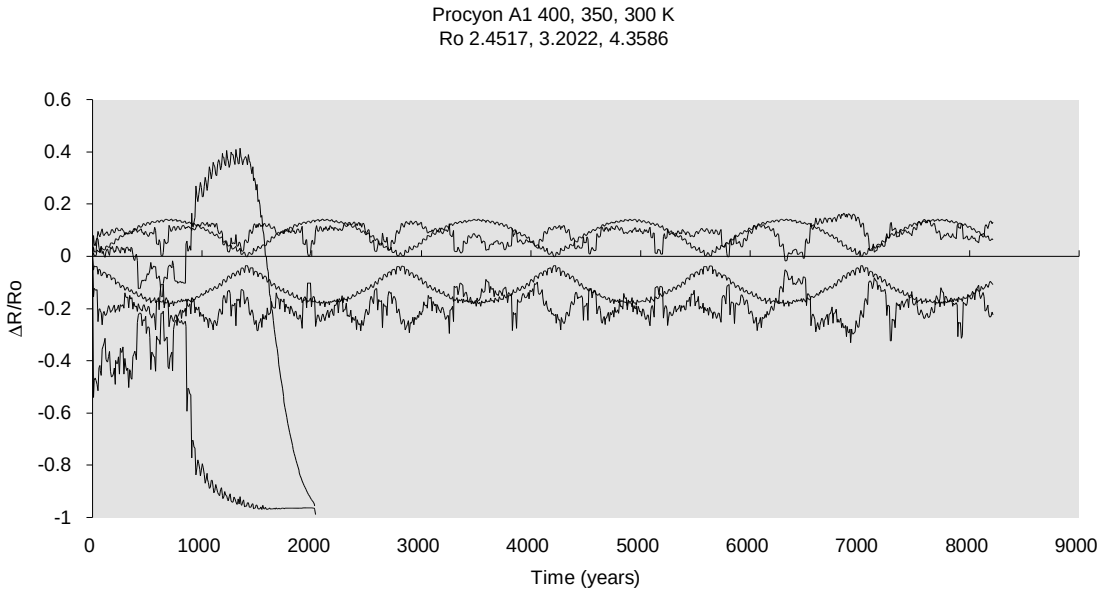

Fig.-9 Procyon A1 Integration Data for T_{eff}=400, 350 and 300^o K (R_o =2.4517, 3.2022, 4.3586 AU) Stable Cycle for 400 ^{o} K, Ragged Pattern for 350 ^{o}, De-Orbit into Primary for 300^o Case.

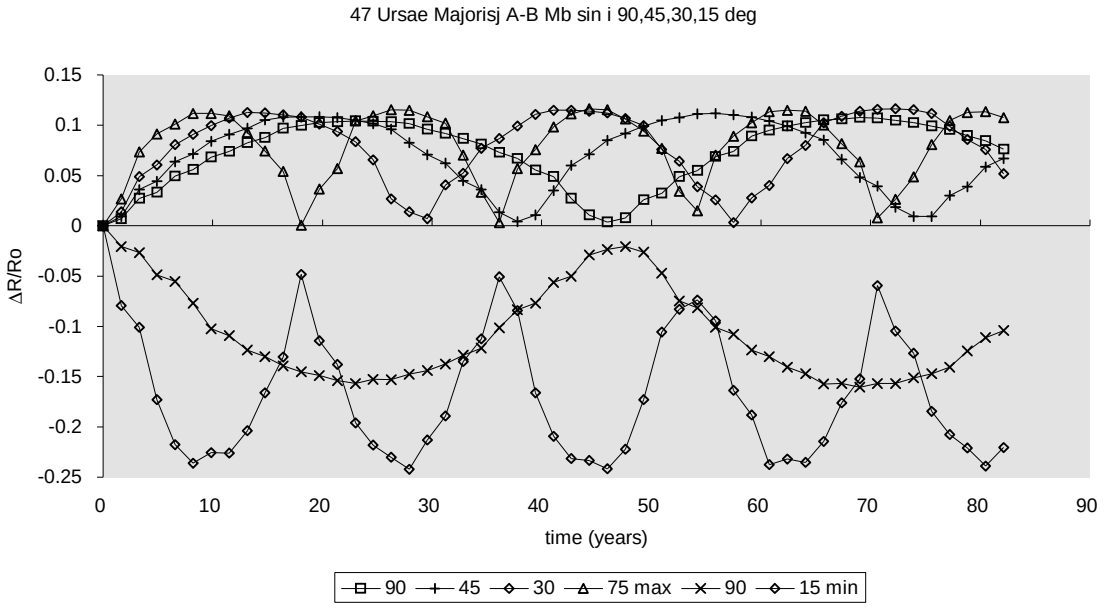

Fig.-10 47 Ursae Majoris Assumed Orbital Plane Line of Sight Inclination

Minimal definitions of a stable orbit could stipulate that 1) the planetary semi-major axis $\mathbf{a}_{pl}$ is constant; 2) changes negligibly; or 3) changes but fractional magnitude withina cycle. Our results adhered closely to the first definition. Eccentricity cycles could be characterized to first order by the following.

$\mathbf{a}_{pl}$ = constant $\quad \mathbf{e} = e(e_o, a, \omega, t) = e_o + \Delta e(a)\, abs\{\sin[\omega_1(a)t + \phi]\}$ $\quad \boldsymbol{\omega}_\mathbf{p} = \omega_1 t$ (9a-c.)

Max **e** is obtained at 180^o rotation of $\boldsymbol{\omega}_\mathbf{p}$. This means that orbits growing more eccentric align axially in the celestial sphere, even if their timing is not the same. Orbits with same **a**, same **e**, have same $\boldsymbol{\omega}_\mathbf{p}$.

Discussion of Dynamic Results

The ER3BP can be modeled several ways. Our approach is to solve the Kepler position problem for the two primary bodies as a function of time and then to integrate the acceleration's exerted on the 3rd body, using a 4th order Runge-Kutta scheme, assuming an inertial frame about stellar barycenter (ER3BP-1). If ordered relative motion such as circular, stable orbits about one primary or another are observed, it is not because such solutions are intrinsic in the formulation. Another approach, discussed in [17], bears close resemblance to the rotating frame of the basic R3BP with no eccentricity: the coordinate system with the contracting and expanding line between the two primaries. This approach (ER3BP-2) leaves to its formulator to account for all the acceleration terms associated with variations in angular rate. In either case, starting with the assumption of M=0 for the 3rd body, approximations have already been made on a trade basis. In the case of the Solar System, $M_{Sun} = 3.3x10^5\ M_E$; the secondary body $M_J = 330\ M_E$.

Our studies examined a dozen stellar systems with co-planar planets, varying initial conditions for temperature zone about star or else orbit **e**, examining periods lasting 10^4 - 10^5 terrestrial years with integration steps of one day or several hundred per planetary revolution. Results provided long term cycles in **e** and ω_p, or else revealed basic orbital instabilities arguing against detection of planets in certain regions of space. We expect that prolonged integration for these cases would seldom extract more information due to numerical uncertainties - and for the intervening effects of real world perturbations.

Real world perturbations can be illustrated by the following example. In our Jupiter-Sun-Mars ER3BP with zero mass Mars in initially circular orbit, our results (compared with α Cen. in Fig. 4) show Mars to experience cyclic variation in **e** from an initial 0 to 0.035, but never reaching its observed current state (.093377; Earth = 0.016722). The system appears bounded, even reminiscent of the Bohr atomic model for electron orbits, where, in this case, planets occupy orbits with "quantum" angular momentum regions, requiring extraneous influences to allow leaps from one state to another. Knowing nothing a priori about Solar System history, we suppose that Earth's or Saturn's presence could bear on the current **e** of Mars; i.e., to suspect that including them as perturbers in the model could lead to the current state. Similarly, one could suspect, that if a terrestrial planet (New Earth) passed the 10^5 year stability test of the ER3BP simulation in orbit around α Cen. A, it could still fail with inclusion of a New Venus or New Mars. Even in the 3-body system, at a certain point the finite mass of the 3rd body becomes significant enough to affect long term stability, if its changes in angular momentum are transferred back and forth to the two primary bodies. In this case, a cycle invisible in the ER3BP could increment a destabilizing process over 10^5 or 10^6 years. Care must also be taken to distinguish this process from cumulative integration errors.

The Solar System and the Sun rotate roughly on the ecliptic (terrestrial) plane, but there are reasons to suspect that binary system planets could be skewed from stellar orbital planes, if the CSDs about the two stars collapse independently. For the planar case, the long term perturbations for a planet orbiting binary A and perturbed by B, the process is incremented through the **e**-cycle by periastron passages. The 80-yr period of α Centauri cycles "New Earth" in 8,000 years or 100 stellar revolutions. The effective exposure time for New Earth to B is an arc segment of its 480-day period, suggesting that a remainder effect could create a high perturbation and low perturbation stellar pass which might cycle over several revolutions. If both stellar and planetary orbital planes are involved, the *planetary* orbital plane is perturbed as well as **e** and the orbital cycles such as **e**-cycle become more complex, if they remain closed cycles.

Sorting Out Data

Whether a general n-body simulation is used, or one of the restricted 3-body systems, a problem that confronts analysts is developing a plan of study based on initial conditions. For an elliptic binary, planetary i.c.s are influenced by f* of the primary bodies, whether at pericentron or apocentron passage. If the stellar temperate zones contact each other, relative stellar position is of concern as well; the angle of initial position with respect to the stellar line of apsides also becomes significant , especially if the initial perturbing effects of the secondary body are considered. Two body relative motion conventions such as

"local circular" or "escape" velocity are good guidelines for estimating periods or near circular initial orbits, but are not exact predictors of orbit behavior.

For stability studies Benest [18-21] developed a phase plane diagram based on inertial velocity and relative position for orbits initialized around primaries (M_A or M_B), normalized in terms of binary system parameters. Using tangential velocity at initialization along the binary periastron line, the i.c.s can be resolved into position coordinate X and velocity component Y. Plots of initially circular orbits constitute two curves, prograde and retrograde; stability bounds defined for a set integration time delineate areas, becoming smaller with increases of duration. For example, Benest obtained stability diagrams for the α Centauri and Sirius systems using ER3BP-2. In effect, for longer and longer test durations (e.g., 10, 100 or 1000 revolutions of the binary pair), the contours become a relief map. Numerical integrations cannot assure stability entirely, but can identify highly stable regions by ascent gradients.

Sirius Problems

Our initial condition sampling did not provide so fine a grid since we examined near circular orbits above and below the radius for $T_{eff} = 400^o$ K. Existence of a planet in the temperate region of α Centauri A appears plausible to the extent that data can be derived from our simulations; similar results were obtained by Benest, Harrington and Holman [22,23]. Our ER3BP-1 analysis found the region between Sirius A and B inhospitable due to dynamic instabilities, however. In Fig. 11, Sirius A1 starts a nominally circular path with significant **e**; after 400 years Sirius B captures it in a cometary orbit (Fig.-12), then it is ejected within 500 years. Even more closely bound orbits ($T_{eff} = 475^o$ in Fig. -13) experience stability problems. Benest considered an eccentric third component ($M>M_J$, 6-year period) for Sirius in this region due to tentative observational reports. Though our simulation results argue to the contrary, this is a well-suited application for such analysis, likely to be repeated as observations come in for other systems.

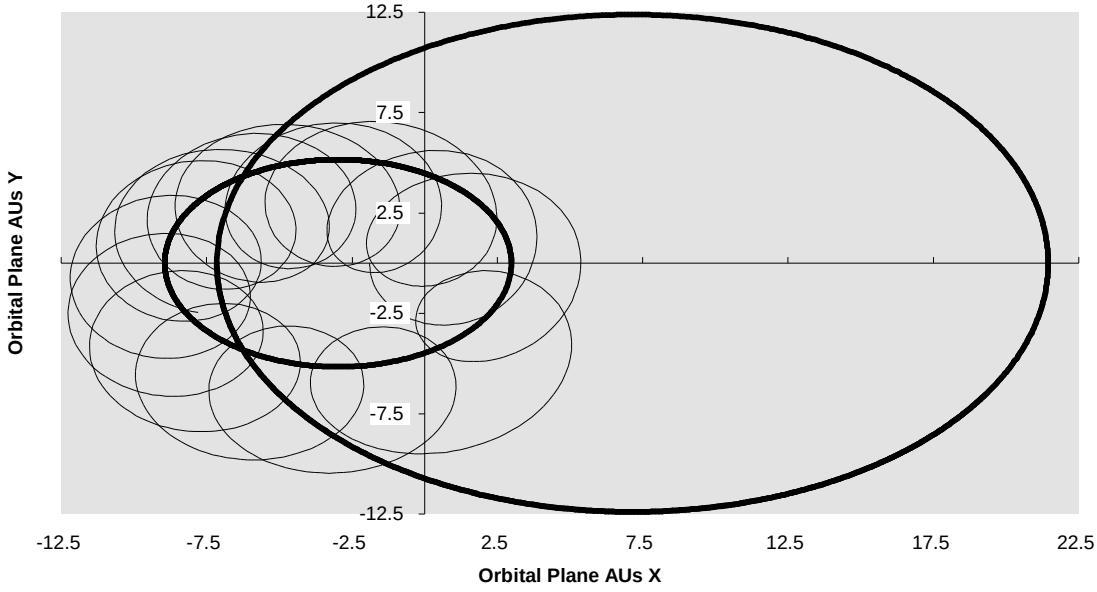

Fig.-11 Sirius A and B, A with A1 Planetary Track at $T_{eff} = 400^o$ K,
Integration for 25,000 days, a* = 30.26 AUs, e* = .50, P* = 49.9 yrs, R_o = 4.88 AU, $T_{eff}=400^o$K
Stellar Mass: M_A = 2.35, M_B = 0.95, Luminosity: L_A = 23, L_B = .00229 (Solar Units)

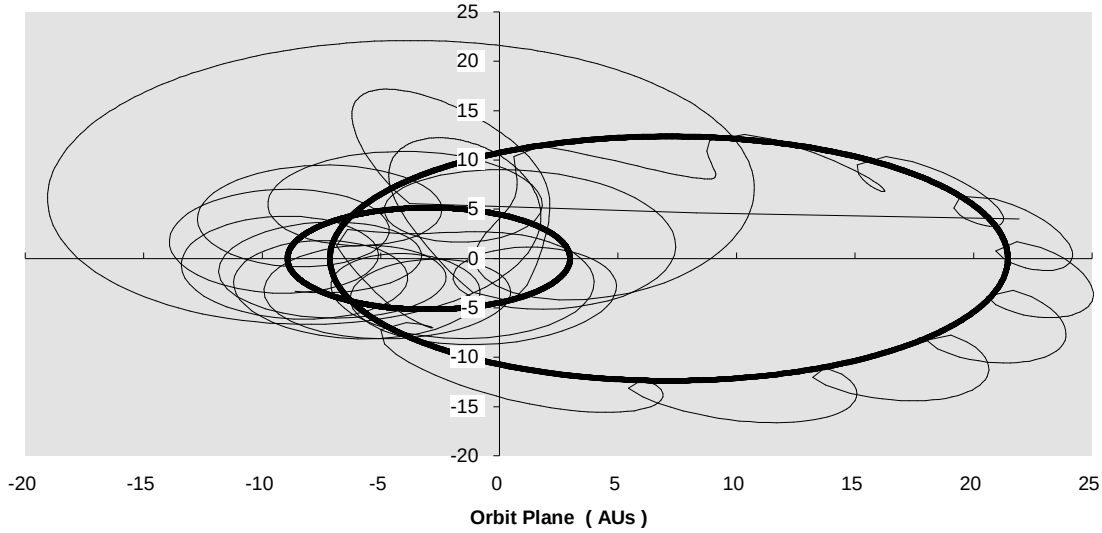

Fig.-12 Sirius A and B, A with Planetary Track Prior to Ejection, Capture by B Prior to Ejection

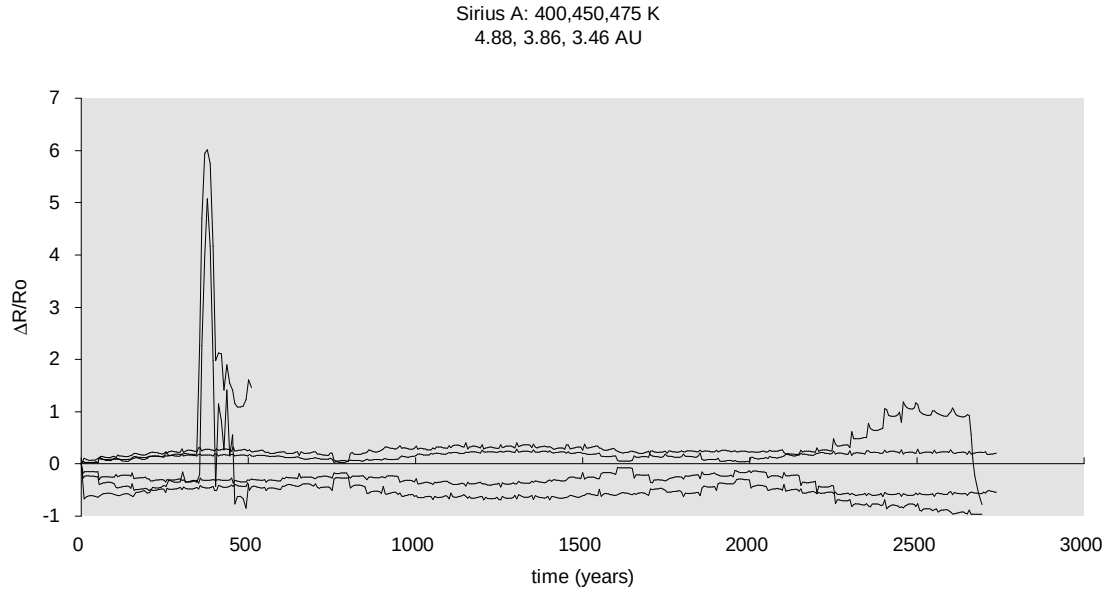

Fig.-13 Sirius A1 Integration Data for T_{eff} = 400°, 450° and 475° K Cases (R_o =4.88, 3.86, 3.46 AU) Capture by B, Then Ejection for 400° after 500 yrs; Ejection of 475° after 2700 yrs.

New Systems with Brown Dwarfs and Jovian Planets

New planetary systems fall midway between the flagrant examples of binary effects illustrated by our 3 nearby star systems, and the muted effects of binary motion inherent in the Jupiter-Sun system. The 70 Virginis system moves into the realm of Venus and Mercury a body more massive than Jupiter ($6.5M_J$ or greater) on a highly eccentric path, composing the only system we examine in which the terrestrial planet orbits both primaries (Fig.-14). The 47 Ursae Majoris case places the jovian mass body roughly at the position of Mars (Fig.-15), the perturbation effects on the planet already apparent in several revolutions. On this account, although we examine its effect on an Earth analog, we would also suspect that it potentially

possesses stable satellites like the Galilean moons. With low system eccentricity this should not be a stability issue. For 70 Virginis B, however, thermal flux is probably too high for habitable satellites, but high system eccentricity makes a moon an interesting dynamics question. With regard to the new systems overall, as shown in Table-3, **e**-variations cycle faster than our other examples.

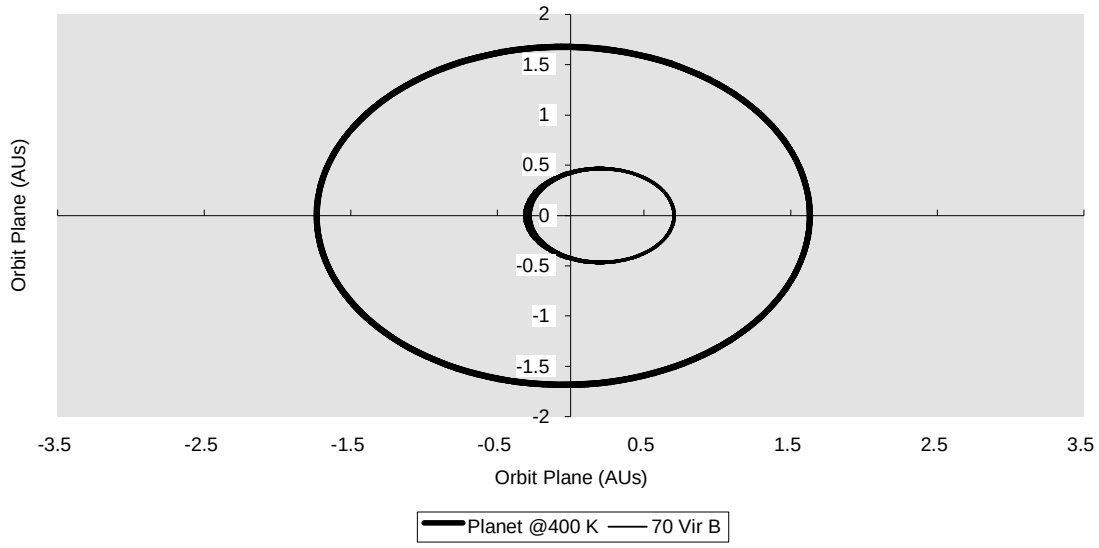

Fig.-14 70 Virginis A, B and Planet at T_{eff}=400^{o} K, Initially Circular Outer Orbit

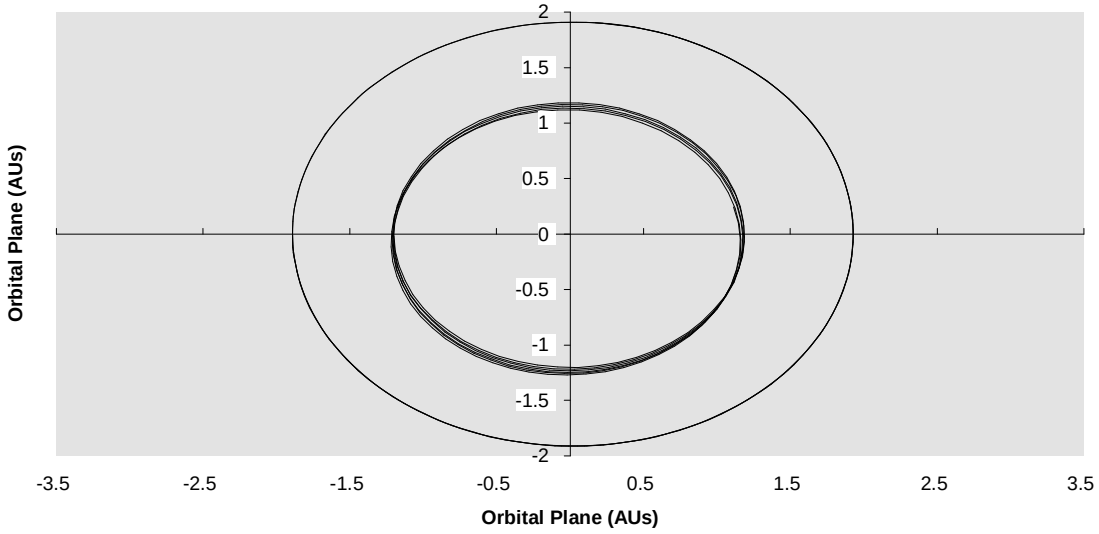

Fig.-15 47 Ursae Majoris A, B and Planet at T_{eff}=400^{o} K, Initially Circular Inner Orbit

For the nominal 70 Virginis 400^{o} case, the longest period (3,500 years) in Fig.-6 also cycles 0. < **e** < 0.3. Fig.-16 displays the variation in the maximum and minimum T_{eff} , deltas of -40 and +70^{o} K. Albedo values for Mars and the Earth are 0.2 and 0.36 respectively which we use to calculate equilibrium surface

temperatures, shown in Fig.-16. It is suspected that human industrial and agricultural processes generating "greenhouse" gases could cause the overall temperature of the Earth to increase several degrees over the next century. Ice ages could have been brought on by similar surface equilibrium temperature changes. Yet expected terrestrial temperature variations are very small in comparison with what would lie in store for the planet orbiting 70 Virginis. A planetary companion to Procyon A (0.< **e** < 0.15 in 1500 years in Tab. -2) would face similar climate changes.

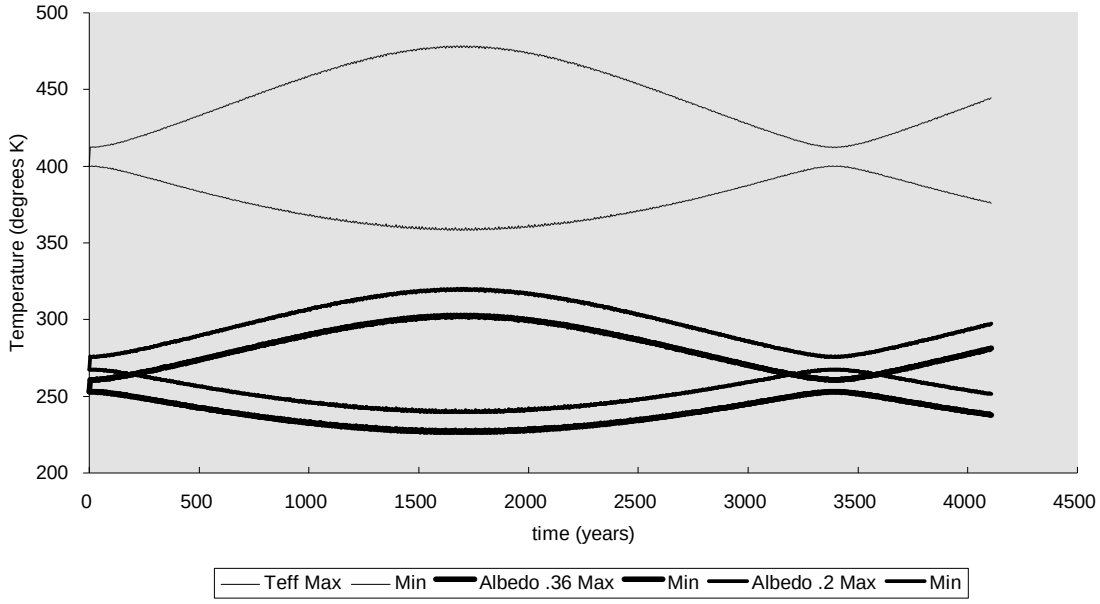

Fig.-16 70 Virginis A1 Temperature Variations with Eccentricity Cycle

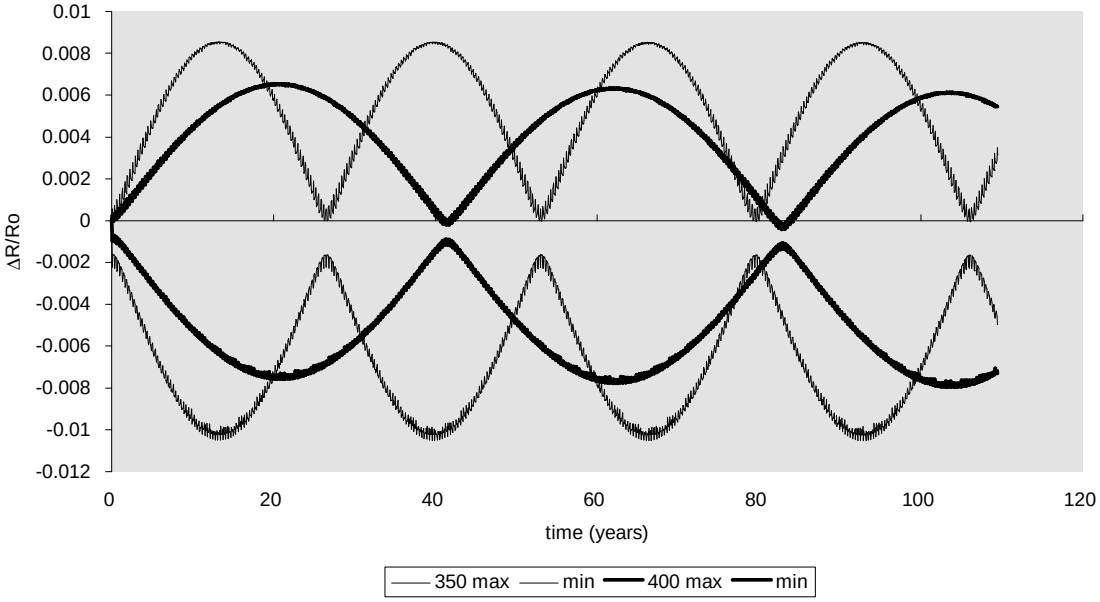

Fig.-17 70 Virginis B Satellite Eccentricity Variations Driven by 117-Day Revolution

Moon over an Eccentric Planet

Many stellar binary systems possess both eccentricity and large mass bodies intruding into the regions of terrestrial planets, but it is difficult to apportion the roles of eccentricity or angular rate changes in causing

instabilities. Jupiter-Sun and 47 U. Maj. possess negligible e*, but similar **e**-cycles are observed on the neighboring small 3rd bodies. 70 Virginis B became the first detected example of a planet or brown dwarf with high e*, followed by an object at 16 Cygni B (e*=.67). Such features lead to questions about how satellite orbits are influenced: whether moons like Io, Europa or Ganymede could remain stable on an amusement park ride. To examine this problem we initialized satellites at similar radii. In this case, at 4.81×10^5 and 6.29×10^5 km, our initial orbits correspond to T_{eff} = 400 and 350° K about a primary with Jupiter's surface radius and T_{eff}*= 1050° K - conjectural values at this date that disregard flux from 70 Vir A, but illustrative all the same. We observe the fastest, but lowest amplitude oscillations of our test sets (Fig. -17). High resolution plots demonstrated that the changes in the sinusoidal curves shown were incremented in discrete steps corresponding to the 117-day orbit of the substellar object (Fig.-18). Although this test does not settle all stability questions, it gives an indication of how surface equilibrium conditions can be affected. Disregarding the thermal contributions of A, shifts in orbital apsides and eccentricity will generate tidal motions in fluids and change polar cap accumulations, generating circulatory systems in what otherwise could be geologically dead bodies locked in synchronous rotation about M_B. In some respects, perhaps disturbances are essential for habitable, terrestrial planets or moons.

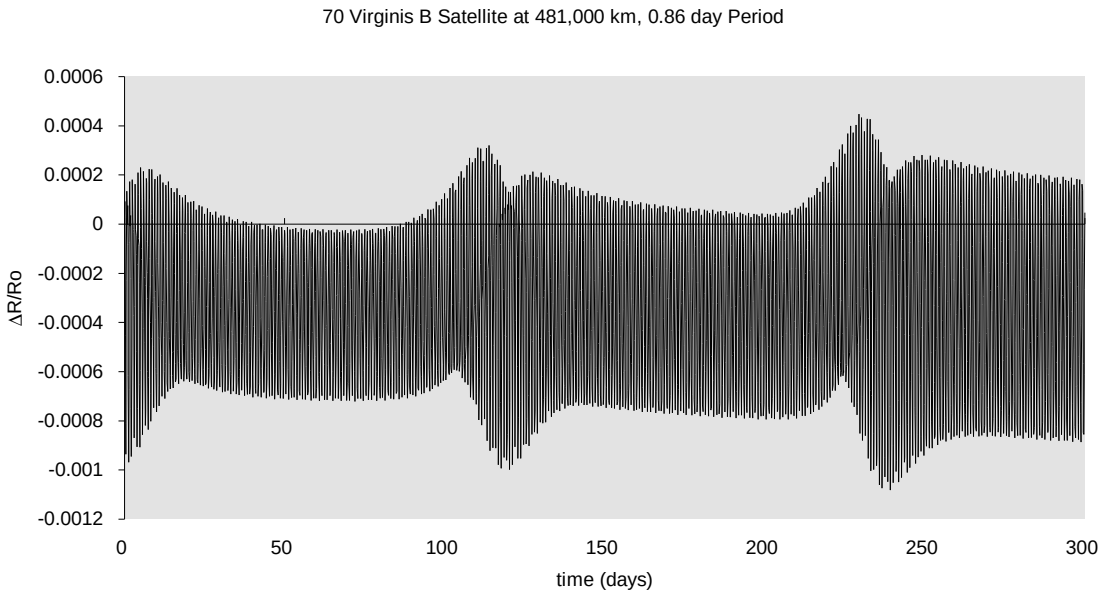

Fig.-18 70 Virginis B Satellite Incremental Variations Driven by 117-Day Revolution - High Resolution

Angular Momentum Bands

"Stable" orbits with precessing ω_p and cycling **e** values imply certain familial relations for orbits of given $\mathbf{a}_{pl}$. For a given $\mathbf{a}_{pl}$ and R_o, initial eccentricity $\mathbf{e}_I$ (vs. $\mathbf{e}_o$) and ω_p place the planet at a particular position on the track of equation 9b. We tested this effect by varyingl $\mathbf{e}_I$ with $R_o = \mathbf{a}_{pl}$. In terms of 2-body mechanics, this initialized orbits at varying initial true anomaly, angular momentum and ω_p. Initial velocities required radial as well as tangential components with respect to M_A. For our nominally circular orbit case at T_{eff}= 400°, in Figs. 3, 6 and 7, **e** varies between near zero and about 0.09 over an 8,000 terrestrial-yr cycle. Fig. 19 shows results for three $\mathbf{e}_I$ values: 0.04, 0.09 and 0.15. These three values are respectively within, at the edge and well beyond the eccentricity bounds of the initially circular case ($\mathbf{e}_I = \mathbf{e}_o = 0.$). In Fig. 19, all three cases are 90 - 100° out of phase with the base case, but the lowest $\mathbf{e}_o$ case did in fact return to near zero value. Some overlap appears in $\Delta R/R_o$ values for 0.04 and 0.09 cases, but the 0.15 case does not flatten out to values below the 0.09 case peak. Some remaining dynamic effects prevent the two low $\mathbf{e}_I$ orbits from coinciding, but in gross terms they are much the same. Allowing for variation in initial true anomaly, the three cycles appear of equal duration.

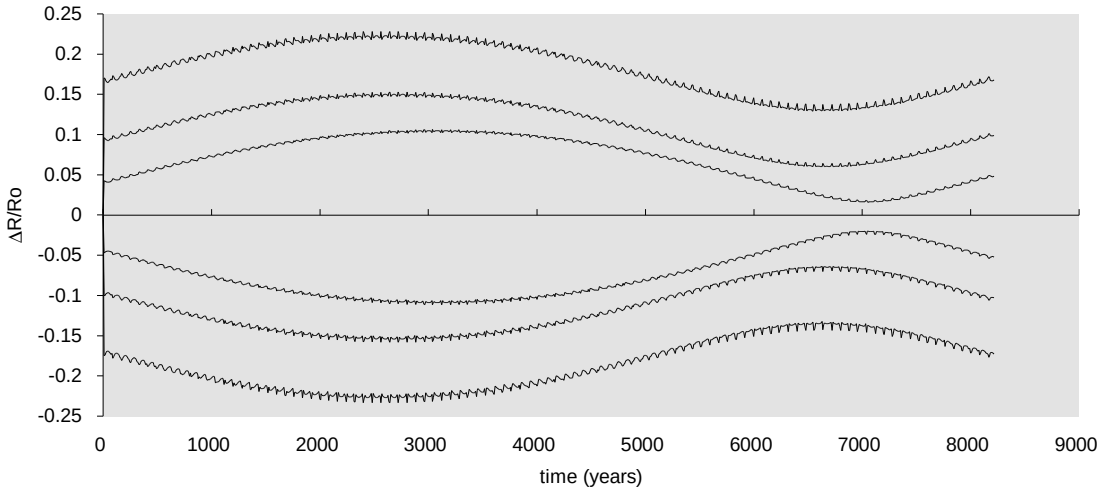

Fig.-19 α Centauri A Planet with Fixed $\mathbf{a}_{pl}$, Varied Initial Eccentricity
Demonstration of Angular Momentum Bands $R_o = \mathbf{a}_{pl} = 1.2468$ AU, $\mathbf{e}_I = .04, .09, .15$

Concluding Remarks

This paper examined planetary motion in star systems dynamically different than our own, yet related to it by features seen in the range of ER3BP behavior. Our concluding remarks qualify those observations and consider the future. Planetary stability can be quantified, but not absolutely, save in the hereafter. A simple definition of a chaotic system is one in which slight i.c. variation results in unpredictable changes in terminal state at fixed time t_f. As the state is advanced from t_N to t_{N+1}, in some instances, little variation occurs as a result of changed i.c.s, until suddenly the system appears to "go off a cliff" or experience catastrophe. For our 3-body studies such cases involve i.c.s leading to 3rd body capture by the 2nd body, collision with M_A or M_B or ejection from the system. When remarkable behaviors are observed, they could be either artifacts of simulation or genuine facets of nature. Cases involving high eccentricity orbits about one or another body with a fixed integration step certainly suffer from losses of "dynamic memory" at close passage. Capture simulations tempt analysts to more detailed simulations, yet already observed outcomes suffice to demonstrate that a planet would not survive for long; increased precision trajectories better illustrate vehicle behavior or how system debris is exchanged or ejected.

To an extent, analysts compare test case solutions generated by different integration schemes or underlying physical assumptions. Long term cyclic behavior exhibited in the RE3BP cases studied are rather spectacular compared to terrestrial or martian adjustments, but could be artifacts of Runge-Kutta integration, depending on the stability of the planetary $\mathbf{a}_{pl}$. Judging by advocates' claims made for symplectic integration [13,14], less excitable algorithms exist. A goal of continued studies is comparison with symplectic and n-body cycles for nominally stable orbits. However, in the 80,000-yr α Cen. A integration shown in Fig.-4, $\Delta\mathbf{a}_{pl}$, derived from sampled extrema each 3,000 days, cycled about $-.0025R_o$ within +/-.0005. Some higher spikes (~.001) were detected.

In substantiating cases with Solar System examples, it is easier to show how stable objects survived than how unstable objects disappeared: e.g., the absence of other natural satellites in the Earth-Moon system. The very notion of i.c.s assumes pre-conditions beyond study scope which perhaps have no means of implementation. In some binary examples, perhaps high eccentricities impose relative velocities too high for adhering collisions among planetesimals. Still, the dynamics of CSDs could tend to dampen **e** growth, or **e** increases, arguably, could be beneficial rather than destructive to planet formation processes. It is

noted that the evolutionary paths of several stars examined (Procyon, Sirius) indicate total Main Sequence lifetimes barely sufficient to fit terrestrial history prior to the development of life; also, thermal flux boundaries drawn need adjustment over billions of years, even in the case of our Sun which has increased its luminosity 40% since ignition of hydrogen fusion. For α Centauri, in which two MS stars afford two separate habitability zones, it appears that α Cen. A, though it more closely resembles the Sun, offers a more perturbed environment for a terrestrial planet than its fainter partner α Cen. B (Tab-2).

Instrumentation and algorithms available ca. 1995 have allowed for discovery of substellar objects plus jovian or greater mass planets, circling rapidly near their primaries, but what about the future and objects discussed here? Prospects are good for continued ground and space-based detector improvements [24-26], but since $M_J = 330\ M_E$, Doppler detection of a New Earth by a Gv star due to primary shifts remains a remote prospect; direct detection appears more likely. To an Earth observer, 1 AU features in Fig.-1 scale to .73 arcsecs, discounting projections of the orbital plane. Visual detection of a stable planet at α Cen. depends on resolving a radiation source separated < 3" from A or B; more distant cases require greater resolving powers. Long wavelength observation should increase a planet's standout against background stellar glare, and instruments coming on line are expected someday to resolve such objects as point sources. Doppler readings direct from a planet emission source, exemplified in Fig.- 1, but viewed at high inclination, should vary about orbital velocity (e.g., +/-28 sin i km/sec). Jovian or terrestrial discs are $\sim 10^{-3}$ or $\sim 10^{-4}$ AU in diameter - consequently less than milli-arcsec features. Spectrographic analyses can commence before genuine pixel imaging of planetary surfaces. CH_4 bands (1.2, 4 microns) in the atmosphere of Gl 229B at 5 parsecs distance have already been used to estimate its mass, T^*_{eff} and surface gravity [15]. Detection of absorption lines at 7, 9.5 or 15 microns respectively for H_2O, O_3 and CO_2 in even fainter prospective objects could give direct comparisons with Earth and evidence of extra-solar terrestrial planets.

In the laboratory, absorption lines give number counts of molecules in an atmospheric column through which a beam of light travels to an instrument. From the depth, width and shift of the line are derived data about the species and other related gases. The readings from a distant planet are a cumulative measure from all visible points on the sphere. In the Earth's case, its visible and IR signature alters as atmospheric clouds, continents, oceans, equatorial jungles and polar ice packs rotate into view; its telluric lines intensify, fade or shift as observed from deep space. We have a theoretical understanding of all these factors, but, to date, little need to observe Earth in this fashion. With our local concerns such as crop yield, emission sources, distributions by latitude, terrestrial remote sensing is not remote enough to reduce all contributions to a point - even for such studies as global warming. In anticipation of extra solar planet comparisons, it is suggested that some interplanetary instruments devote time observing Earth for a better calibrated "point source" view.

Acknowledgments

The author thanks participants at the June 1996 Planetary Formation in the Binary Environment Conference (State University of New York, Stony Brook) where portions of this report were presented; their observations provided guidance and better astrophysical perspective. Crimean Astrophysical Observatory astronomers Nikolai Gor'kavyi and Tanya Taidakova monitored progress and provided encouragement via e-mail during a joint project.

References

[1] Kelly, W. D., "Planetary Motion about Nearby Binary Star Systems with Restricted Elliptic 3-Body Motion", *Journal of the Astronautical Sciences*, April-June 1986, v. 34 (2).

[2] Kelly, W. D., "Planetary and Dust Particle Orbits about Binary Stars: Long Term Trajectories and Radiation Effects", AIAA 88-4261, AIAA/AAS Astrodynamics Conference Proceedings, Aug. 1988.

[3] Marcy, G.W., Butler, R. P., "A Planetary Companion to 70 Virginis", *Astrophysical Journal Supplement*, 20 June 1996.

[4] Marcy, G. W., Butler, R. P., "A Planetary Companion to 47 Ursae Majoris", Ibid.

[5] Beckwith, S., Sargent, A., "The Occurrence and Properties of Disks around Young Stars", *Protostars and Planets III* (J. L. Lunine, ed.), pp. 521-541, Univ. of Arizona Press, 1994.

[6] Beckwith, S., Sargent, A., "Circumstellar Disks and the Search for Neighboring Planetary Systems", *Nature*, 1996, Vol. 383, p. 139, 12 Sept. 1996.

[7] Bowers, R., Deeming, T., *Astrophysics I: Stars*, Jones and Bartlett, Boston , 1984.

[8] Swihart, T. L., *Astrophysics and Stellar Astronomy*, John Wiley & Sons, New York, 1968.

[9] Haisch, B. , Johnson, H. et al.,"Creation of Photometric Star Catalogs Using UBV Data and Model Stellar Atmospheres", *Journal of the Astronautical Sciences*, 1983, v. 31, n. 4, pp 473-506,

[10] Burnham, R. Jr., *Burnham's Celestial Handbook*, Vols. 1-3, Dover Press, New York, 1978.

[11] Dibon-Smith, R., *Starlist 2000: A Quick Reference Star Catalogue for Astronomers*, John Wiley, New York, 1992.

[12] Butler, R P., Marcy, G. W., Williams, E., McCarthy, C., Dosanjh, P., "Attaining Doppler Precision of 3 m/s", *Pub. Astron. Soc. of the Pacific*, v. 108, pp. 500-509, June 1996.

[13] Yoshido, H., "Recent Progress in the Theory and Application of Symplectic Integrators", 1993, *Celestial Mechanics*, v. 56, pp 27-43.

[14] Taidakova, T., "A New Stable Method for Long-Time Integration in an N-Body Problem", 1996, pre-print, Crimean Astrophysical Observatory, Ukraine.

[15] Kulkarni, S. R., et al., "Infrared Spectrum of the Cool Brown Dwarf Gl 229B", *Science*, v. 270, 01 Dec. 1995, pp. 1478-79.

[16] Kasting, J., Whittet, D., Sheldon, W., "Effect of UV Radiation on Planetary Habitability", 26th Lunar and Planetary Science Conference Abstracts, LPI/USRA, Houston, 1996.

[17] Szebehely, V., *Theory of Orbits: The Restricted Problem of Three Bodies*, Academic Press, New York, 1973.

[18] Benest, D., "Stable Planetary Orbits around One Component in Nearby Binary Stars", 1988, *Celestial Mech*., Vol. 43, 47.

[19] Benest, D., "Planetary Orbits in the Elliptic Restricted Problem, I - The Alpha Centauri System", 1988, *Astronomy and Astrophysics*, v. 206, p. 143.

[20] Benest, D., "Stable Planetary Orbits around One Component in Binary Stars, II", 1993, *Celestial Mechanics*, v. 56, pp. 45-49.

[21] Benest, D. "Planetary Orbits in the Elliptic Restricted Problem, II - The Sirius System",1989, *Astronomy and Astrophysics*, v, 223, p. 361.

[22] Harrington, R. S., "Planetary Orbits in Binary Stars", *Astronomical Journal*, v. 82, n. 9, pp. 753-56, Sept. 1977.

[23] Holman, M., Wiegert, P., "Long Term Stability in Binary Systems", Presentation - Planetary Formation in the Binary Environment, SUNY Conference, 16-18 June 1996.

[24] Burke, B. F. (ed.), et al., "TOPS - Toward Other Planetary Systems", NASA Solar System Exploration Division Report, 1992.

[25] Traub, W. A., Carleton, N. P., Porro, I. L., "A Search for Planets in Nearby Binary Stars Using a Ground-Based Interferometer", *Journal of Geophysical Research - Planets*, pre-print, 1996.

[26] Baldwin, J.E. et al., "The First Images from an Optical Aperture Synthesis Array: Mapping of Capella with COAST at Two Epochs", *Astronomy and Astrophysics*, v. 306, p. 13, Feb. 1996.

Table-1 Parameters for Nearby Binary Stars and Stars with Newly Discovered Planets

(Computer Simulation Values - Data Include Jupiter - Sun Model)

System Name	Stellar Mass M*	Spectr. Class	Surface Temp. (^oK)	Stellar Radius	Luminosity L*	Mean Separation (AUs)	Binary Eccen-tricity	Binary Period (yrs)
----------Binary Stars ----------								
α Centauri A	1.1	G2v	6205	1.07	1.50	23.4395	0.52	79.92
B	0.85	K1v	4175	1.22	0.40	"	"	"
Procyon A	1.7	F5iv	6850	1.785	5.8	16.029	0.4	40.65
α Canis Min B	0.65	WD	6238	0.02	.0023	"	"	"
Sirius A	2.35	A1v	9630	1.8	23	30.26	0.5	49.98
α Canis Maj B	0.95	WD	8673	0.021	0.00229	"	"	"
---------- Stars with Large Planets or Brown Dwarfs ----------								
47 Ursae Maj A	0.7788	G0v	5701	1.1	1.4	2.1	.01 -.15	3.0
(2.3 M_J) B	$2.18x10^{-3}$		-	0.1	-	"	"	"
70 Virginis A	1.351	G2.5v	6079	1.8	2.9	0.43	0.38	117 d.
(6.5 M_J) B	$5.985x10^{-3}$		-	0.1	-	"	"	"
---------- Solar Model ----------								
Sun A	1.0	G2v	5862	1.0	1.0	5.2	0.0484	11.8922
Jupiter B	$9.85x10^{-4}$		125	0.1	0.0...	"	"	"
----------Other New Systems----------								
51 Pegasi A	1.0	G2v	~5800	1.0	1.0	0.0512	0.00	4.229 d.
(0.5 M_J) B	$4.37x10^{-4}$		-	0.1	-	"	"	"
Gliese 229 A	.425	M1v	3800	.562	.0582	~40.	?	~400
B	.0019		1000	0.1	-			
ρ Cancri[1] A	.8150	G8v	5400	-	-	0.11	0.00	14.76 d.
(0.8M_J) B			-	0.1	-	"	"	"
16 Cygni B	1.026	G2.5v	5700	-	-	1.701	0.67	804 d.
(1.5M_J)			-	0.1	-	"	"	"
HD 114762 A	.8105	F9v	~6000	1.	-	0.34	0.35	0.23
(9M_J) B			$1\text{-}3x10^3$	0.1		"	"	"
---------- Circumstellar Disk with Possible Proto Planet(s)----------								
β Pictoris	2.0	A5v	8220	1.4	7.9	-	-	-
----------Pulsar with Terrestrial Sized Planets ----------								
Pulsar PSR 1829-10	(Two bodies of mass 2.8M_E and 3.4M_E).							

0.5 M_J < Jovian Planets < 13M_J, e ~ 0.

Jupiter M_J = .001 M_{SUN} = 330 M_E

Brown Dwarfs : e >> 0, Condensation from nebula vs. protoplanetary disk.

13M_J < M < 80 M_J deuterium fusion internal heating.

Main Sequence Hydrogen Fusion Ignition M* > 0.08 M_{SUN} , faintest M stars.

Substellar spectroscopic masses (M_B sin i)in binaries above are minima (i = 90^o).

Inclination of orbit plane normal to LOS .

Table -2 Planetary Orbits at Control Volume Temperature Radii from Binary Stars Elliptic Restricted 3-Body Problem Results

Star System Component	T_{eff} (R_o) Temperature (^oK)	Nominal Radius R_o (AUs)	2-Body Period (days)	Ejection (yrs)	Eccentricity Cycle Period (10^3yrs)	Magnitude ($\Delta R/Ro$)
α	400	1.2468	484		8.0	0.08, -0.09
Centauri	350	1.6285	724		5.0	0.11, -0.12
A	300	2.2165	1,149		2.6	0.12, -0.15
	275	2.6368	1,492	-	1.8	0.13
	250	3.1918	1,985	-	-	-
	225	3.9405	2,724	2,500	-	-
α Centauri B	400	0.6438	204	-	15.8	0.05, -0.05
Procyon -	400	2.4517	1,075.4	-	1.5	0.12, -0.18
α Canis	350	3.2022	1,605	-	-	-
Minoris A	300	4.3586	2,549	2,000	-	-
Sirius -	475	3.462	1,535	2,700	28	~0.2, -0.3
α Canis	450	3.875	1,805	-	1.0	~0.3, -0.6
Majoris A	400	4.882	2,870	550	-	-0.15, -0.6
Sun with	400	1.000 (Earth)	365		180	0.023, -0.023
Jupiter	327.5	1.518 (~Mars)	684		88	0.035, -0.035
	250	2.606	1,536	-	>8.0	>0.05
	200	4.072	3,001	-	4.5	0.065
		[ejections around Jupiter @5.2 AU]				
(RE3BP)	150	7.239	7,113	-	1.0	0.17, -0.23

Table -3 M_b sin i Contours for Spectroscopic Binary Systems: ER3BP Results

Star System Component	T_{eff} (R_o) Temperature (^oK)	Nominal Radius R_o (AUs)	2-Body Period (days)	Ejection (yrs)	Eccentricity Cycle Period (yrs)	Magnitude ($\Delta R/Ro$)	LOS Inclin (deg)
70	400	1.7332	717	-	3450	0.23, -0.3	90
Virginis A				-	2400	0.24, -	45
				-	1500	0.25, -	30
				-	400	0.25, -0.4	15
70 Vir. B	"400"	481,000 km	0.862	-	41	.0065, -.007	90
	"350"	629,000 km	1.287	-	24	.008, -.0105	90
[Satellite T_{eff} for B as only radiation source, T^*_{eff} =1050 K, jovian surface radius]							
47	400	1.204	547	-	43.8	0.12. -0.15	90
Ursae				-	30	0.12	45
Majoris A				-	18	0.12, -0.24	15

Bibliography

[2] Alfriend, K. T., Rand, R. H., "Stability of Triangular Points in the Elliptic Restricted Problem of Three Bodies", AIAA Journal, vol. 7, n. 6, pp. 1024-1028, June 1969.
[3] Black, D. C., "A Simple Criterion for Determining the Dynamical Stability of Three Body Systems", The Astronomical Journal, v. 87, n. 9, Sept. 1982, pp. 1333-1337.
[5] Burnham, R. Jr., *Burnham's Celestial Handbook*, Vols. 1-3, Dover Press, New York, 1978.
[6] Danby, J. M. A., "Stability of Triangular Points in the Elliptic Restricted Problem of Three Bodies", The Astronomical Journal, v., 69, n. 2, pp. 165-172, Mar. 1964.
[9] Heppenheimer, T. A., "Outline of a Theory of Planet Formation in Binary Star Systems", *Icarus*, v. 22, pp. 436-447, 1974.
[10] Gor'kavyi, N. N., Fridman, A. M., *Physics of Planetary Rings* - Celestial Mechanics of a Continuous Medium, Moscow, Russian ed., Nauka Press, 1994, 348 p. (Engl. ed., Springer-Verlag, 1996, in press).
[24] Hale, Alan, "On the Nature of the Companion to HD114762", PASP, 107, 22-26, 1995 January.
[25] Saumon, D., Hubbard, W., Burrows, A., Lunine, J. I., et al., "A Theory of Extrasolar Giant Planets", Ap. J., 460, 993-1018, 01 April 1996.
[26] Guilot, T., Burrows, A., Hubbard, W., Lunine, J., Saumon, D., "Giant Planets at Small Orbital Distances", Ap. J. Letters, 459, L35-L38, 01 March 1996.
[30] Mundy, L. G., et al., "Imaging the HL Tauri Disk at λ= 2.7 mm with the BIMA Array", Ap. J. Letters, 464, L169-173, 20 June 1996.
[31] Beust, H., Morbidelli, A., "Mean-Motion Resonances as a Source for Infalling Comets toward β Pictoris", Icarus, 120, 358-370, 1996.
[32] Beckwith, S., Sargent, A., "The Occurrence and Properties of Disks around Young Stars", *Protostars and Planets III* (J. L. Lunine, ed.), pp. 521-541, 1993,. Univ. of Arizona Press.
[33] Basri, G., Bertout, C., "T Tauri Stars and their Accretion Disks", *Prototsars and Planets III* (J. Lunine, ed.), 543-566, 1993, Univ. of Arizona Press.
[34] Wolk, S. J., Walter, F. M., "A Search for Protoplanetary Disks around Naked T Tauri Stars", The Astron. Journal, Vol. 111, No. 5, pp. 2066-2076, May 1996.
[35] Jensen, E., Mathieu, R., Fuller, G., "The Connection between Submillimeter Continuum Flux and Separation in Young Binaries", Ap. J., 458, 312-326, 10 February 1996.
[37] Lin, D., Papaloizou, J., "On the Tidal Interactions between Protostellar Disks and Companions", *Prototsars and Planets III* (J. Lunine, ed.), 749-835, 1993, Univ. of Arizona Press.

Baldwin, J.E. et al., "The first images from an optical aperture synthesis array: mapping of Capella with COAST at two epochs", Astronomy and Astrophysics, v. 306, p. 13, Feb. 1996.

We present the first aperture synthesis maps obtained using closure phase techniques with a separated-element optical interferometer. Maps of the double-lined spectroscopic binary Capella ({alpha} Aurigae) were obtained at 830nm with threeelements of the Cambridge Optical Aperture Synthesis Telescope (COAST) in September 1995. These maps show clearly themilliarcsecond orbital motion of the system over a 15 day interval. The image quality is comparable to that of VLBI images obtained using similarly sparse radio synthesis arrays, and the location and motion of the binary components are in excellent agreement with the predictions of the latest set of orbital elements. These data demonstrate for the first time the feasibility of operating long-baseline optical/near-infrared interferometers for high-dynamic range high-resolution imaging.